

ORIGINAL ARTICLE

Functional characterisation of bioactive peptide derived from terrestrial snail *Cryptozona bistrialis* and its wound-healing property in normal and diabetic-induced Wistar albino rats

Selvakumari Ulagesan¹ | Kamatchi Sankaranarayanan¹ | Amutha Kuppusamy²

¹Department of Energy and Environment, National Institute of Technology, Tiruchirappalli, India

²Department of Biotechnology, Vels University, Chennai, India

Correspondence

Dr. S Ulagesan, Department of Energy and Environment, National Institute of Technology, Tiruchirappalli 620 015, Tamil Nadu, India.
Email: ula.selva@gmail.com

Abstract

A peptide might be an exciting biomaterial or template for the development of novel wound-healing agents. In this report, it was isolated from the terrestrial snail *Cryptozona bistrialis* by enzymatic digestion and was evaluated for its in vitro wound-healing activity in NIH/3T3 mouse fibroblasts cell line and in vivo wound-healing activity in normal and diabetic-induced Wistar albino rats. The *C. bistrialis* protein was digested by the papain enzyme, and 21.79 kDa peptide (Cb-peptide) was purified by reversed-phase high-performance liquid chromatography and identified by MALDI (matrix-assisted laser desorption/ionization)-TOF analysis. The isolated Cb-peptide was characterised by various analytical methods. The peptide demonstrated a capacity to prevent the development of pathogenic bacterial and fungal cultures and proved that it promotes significant wound-healing activity in the wound scratch assay method by rapid cell migration and closure of wound. Isolated Cb-peptide was lyophilised and formulated to ointment and analysed for in vivo wound-healing activity in normal and diabetic (alloxan monohydrate)-induced Wistar albino rats. Cb-peptide ointment-treated groups showed a greater degree of wound healing and early and complete period of epithelialisation in normal and diabetic-induced Wistar albino rats. Cb-peptide ointment-treated groups showed significant excision and incision wound-healing activity. A conclusion was reached that the peptide isolated from *C. bistrialis* showed greater wound-healing activity compared with vehicle control and standard control.

KEYWORDS

antimicrobial activity, bioactive peptide, diabetic wound healing, in vitro wound healing, mollusks

1 | INTRODUCTION

Wound healing is a complex process of restoring impaired cells and tissues back to their normal state and occurs as a cellular response to injury, which also involves the activation of fibroblasts, endothelial cells, and macrophages. It also involves a well-orchestrated integration of biological and molecular event of cell migration, cell proliferation.¹ A major factor that influences wound healing is bacterial

and fungal infection. When a wound is infected by bacteria and fungus, it produces inflammation and accumulation of fluid, which interferes with the healing process. In addition, bacteria toxins cause tissue damage and delay fibroplasias as well as collagen synthesis.²

Consequently, the healing process is delayed in patients who are affected with diabetes mellitus. Diabetes mellitus is a disorder provoked by chronic hyperglycaemia and generates many complications like foot ulcers and poor wound

Key Messages

- a wound refers to an injury that damages the dermis of the skin; diabetes mellitus and microbial infection is an important factor that affects the healing process of the wound and leads to life-threatening complications
- consequently, there exists a need for a new agent that may be useful in proper wound management, and with regards to this, a bioactive peptide from gastropod is being investigated
- the terrestrial snail *Cryptozonia bistrialis* peptide demonstrated significant activity against pathogenic bacterial and fungal cultures
- in vivo wound-healing activity was performed in normal and diabetic-induced Wistar albino rats; peptide ointment showed significant wound-healing activity in normal and diabetic-induced Wistar albino rats

healing.³ Diabetic wounds are slow, non-healing wound that can persist for weeks despite adequate and appropriate care. Such wounds are difficult and tough to manage. In the final stage of wound healing, fibroblast proliferation involves the restoration of structure and function in the wound site.⁴ There is a clinical need for new, more effective treatments for chronic wounds in diabetic patients.

Management of chronic wound involves the use of antibiotics, anti-inflammatory agents or combination of both, but some of these drugs are associated with unwanted side effects, hence the need for other alternatives without producing toxicity.⁵ Much research is aimed at trying to find ideal clinical wound-healing biomaterials. Small molecules with low cost and function to promote production of endogenous wound-healing agents are especially excellent candidates. There is mounting interest in the therapeutic potential of bioactive peptides, which collectively present plenty of bioactivities. Peptides are interesting biomaterials with excellent wound-healing properties. Antimicrobial peptides have attracted much research interest because of their biochemical diversity and broad specificity with regards to antiviral, antibacterial, antifungal, anti-protozoan parasites, and even anti-tumoural or wound-healing effects.⁶

Mollusks are an abundant and significant group in the trophic chain of the animal kingdom. There are more than thousands of bioactive compounds discovered in mollusks. They include peptide, sterols, terpenes, polypropionate, nitrogenous compounds, macrolides, fatty acid derivatives, miscellaneous compounds, and alkaloids.⁷ Many bioactive compounds have been investigated predominantly for their antimicrobial, cytotoxic, anti-tumour and anti-inflammatory, anti-leukaemic, antineoplastic, and antiviral properties of mollusks.^{8–12} Among the mollusks, gastropods,

including snails and slugs, represent the most abundant class. Snails in particular are successful animals from an evolutionary point of view due to their capacity to adapt to different environments and to reach dry land.¹³ For centuries, snails have been used both as a food and as a treatment for variety of medicinal conditions. They have been used sporadically as skin treatments since the time of ancient Greeks; Hippocrates reportedly recommended the use of crushed snails to relieve inflamed skin and heal the wound. The mucus collected from snail is rubbed onto the skin to treat dermatitis, inflammations, calluses, acne, and to promote wound healing.¹⁴

Enzymatic hydrolysis of proteins involves the cleavage of peptide bonds, resulting in the breakdown of proteins to peptides and amino acids.¹⁵ The peptides derived from mollusks are easy to obtain, cheap, and safe without any adverse effects in comparison with their synthetic counterparts. From this perspective, the present study was designed to isolate a peptide from the terrestrial snail *Cryptozonia bistrialis*, which was then evaluated for wound-healing activity in normal and diabetic-induced Wistar albino rats.

2 | METHODS

Live *C. bistrialis* (land snails) specimens were collected from Thirumazhisai agricultural field, Chennai, India. They were identified by Dr. R. Venkitesan, Scientist C, Zoological Survey of India, Chennai, India. The study was registered under registration number LM-551, *C. bistrialis* (Beck, 1837). The collected snails were brought to the laboratory, and the shells were broken, and the soft body was separated and stored at -20°C until use.

2.1 | Preparation of protein hydrolysate

The proteolytic digestion was performed on the protein of *C. bistrialis* using the method described by Je et al.¹⁶ *Cryptozonia bistrialis* was digested by the papain enzyme, and the protein hydrolysate of *C. bistrialis* was separated into 2 filtrates based on molecular weight—low (<10 kDa) and high (>10 kDa)—using the Amicon Ultra centrifugal device and 10 kDa cut-off membrane, and both filtrates were screened against antimicrobial activity. An activity-rich high molecular weight (>10 kDa) fraction was further applied onto a reversed-phase high-performance liquid chromatography (RP-HPLC) C-18 column; 60 different fractions were collected, and the antimicrobial activities of all fractions were evaluated. Activity-rich fractions were pooled together and were analysed using MALDI (matrix-assisted laser desorption/ionization)-TOF/TOF analysis. The peptide was further characterised using the UV-Vis, fluorescence, circular dichroism (CD) spectrophotometer.

2.2 | MALDI-TOF analysis

The peptide derived from the papain digestion of *C. bistrialis* (Cb-peptide) was analysed using an UltraFlex III MALDI-TOF/TOF (Bruker Daltonics TESCANA, USA, Inc.) precisely calibrated with peptide calibration standard II. A 1 mL sample was mixed with 3 mL of matrix solution (1% [w/v] *a*-cyano-4 hydroxycinnamic acid, 3% [v/v] trifluoroacetic acid, and 50% [v/v] acetonitrile) and applied onto a MALDI target plate (1 mL in duplicate). After crystallisation at room temperature, samples were analysed using a spectrometer operated in reflector mode for mass spectrometry (MS) acquisitions and lift mode for tandem MS (MS/MS). Peptide sequence identification was achieved by Masscot search, similar to bioactive peptides.

2.3 | UV-Vis spectrophotometer

The Cb-peptide was analysed using a UV-1800-Shimadzu spectrophotometer with quartz cells of 1 cm path length. The corresponding buffers were used as reference for the measurements.

2.4 | Fluorescence spectrophotometer

The steady state fluorescence spectroscopy was performed using the Cary Eclipse Spectrometer. Fluorescence was recorded with λ_{ex} wavelength at 280 nm (slit width 5 nm).

2.5 | Circular dichroism spectrophotometer

CD spectra of the Cb-peptide were carried out using a JASCO J-715 spectropolarimeter (JASCO Corp., Tokyo, Japan). The far-UV (240-190 nm) spectra of the peptide were obtained using 0.1 cm path length quartz cells. All measurements were taken a minimum of 3 times to ensure reproducibility. The spectra were analysed using the Dichro-web fitting to 4 structural parameters: α -helix, β -sheet, β -turn, and random coil.

2.6 | Scanning electron microscopy

Scanning electron microscopy (SEM) was used to study the morphology of the films of Cb-peptide transferred to solid surfaces. The protein solution was allowed to reach the equilibrium surface tension, and then, the film was transferred onto cleaned solid substrates using the Langmuir-Schafer film transfer technique and was characterised using SEM. A thin layer of gold (200 Å) was sputtered on these samples, and SEM studies were undertaken using a VEGA3 model SEM from TESCANA.

2.7 | Antimicrobial activity of the peptide isolated from *C. bistrialis*

The isolated Cb-peptide was evaluated for its antibacterial and antifungal activity by broth dilution method¹⁷

(minimum inhibitory concentration) against six human pathogenic bacterial strains and four pathogenic fungal strains.

The bacterial strains include *Staphylococcus aureus* and *Micrococcus luteus*, *Pseudomonas aeruginosa*, *Proteus vulgaris*, *Serratia marcescens*, and *Hafnia alvei*.

The pathogenic fungal strains included *Candida albicans*, *Aspergillus fumigatus*, *Penicillium chrysogenum*, and *Mucor racemosus*.

These pathogenic cultures were obtained from the King Institute of Preventive Medicine, Guindy, Chennai, India. The organisms were periodically sub-cultured and maintained in respective media at 4°C.

2.8 | In vitro wound-healing activity of Cb-Peptide

2.8.1 | Cell line and culture

An NIH/3T3 mouse fibroblast cell line was obtained from the National Centre for Cell Sciences (NCCS), Pune, India. The cells were maintained in minimal essential media supplemented with 10% Fetal Bovine Serum (FBS), penicillin (100 µg/mL), and streptomycin (100 µg/mL) in a humidified atmosphere of 50 µg/mL CO₂ at 37°C.

2.8.2 | Cytotoxicity activity (MTT assay)

The cytotoxicity of Cb-peptide on NIH/3T3 (mouse fibroblast) was determined by the MTT assay.¹⁸ After 48 hours of incubation, the cell reached the confluence. Cells were cultured in a 96-well plate with at least 3 empty wells. At least 3 wells should be absent of media for 12 hours for the control condition, grown in sub-confluent monolayers. At the time of the experiment, 150 µL of media per a well was added. Then, cells were incubated in the presence of various concentrations of the Cb-peptide in 0.1% Dimethyl sulfoxide (DMSO) for 48 hours at 37°C. After removal of the sample solution and washing with phosphate-buffered saline (pH 7.4), 200 µL/well (5 mg/mL) of 0.5% 3-(4,5-dimethyl-2-thiazoly)-2,5-diphenyl-tetrazolium bromide cells (MTT) phosphate-buffered saline solution was added. After 4 hours of incubation, 0.04 M HCl isopropanol was added. Viable cells were determined by the absorbance at 570 nm. Measurements were taken, and the concentration required for a 50% inhibition of viability (IC₅₀) was determined graphically. The effect of the Cb-peptide on the proliferation of NIH/3T3 was expressed as the percentage of cell viability using the following formula:

$$\text{Percentage of cell viability} = \frac{A_{570} \text{ of treated cells}}{A_{570} \text{ of control cells}} \times 100$$

2.8.3 | Wound scratch assay test

The Cb-peptide was analysed for its wound-healing activity in the NIH/3T3 mouse fibroblast cell line.¹⁹ NIH/3T3 cells were seeded in 24-well plates at a concentration of 3×10^5 cells/mL, cultured in a fibroblast media containing 5% FBS and grown to confluent cell monolayer. The media were

pipetted out and discarded; a small area was then scratched using a 200 μL pipette tip, and the cells were then rinsed with PBS to remove the loose debris of the cells. Fibroblast media with serial dilution of different concentrations of Cb-peptides at 3.12, 6.25, 12.5, 25, 50, and 100 $\mu\text{g}/\text{mL}$ were replaced, and the plates were incubated at 37°C and 5% CO_2 . The distance between 2 layers of cells that were scratched by the pipette tip was then inspected microscopically at 24, 48, and 72 hours. As the NIH/3T3 cells migrate to fill the scratched area, images were captured with a digital camera attached to the microscope and computer system. The experiments were performed in triplicates.

2.9 | In vivo wound-healing activity of Cb-Peptide

2.9.1 | Ethical committee clearance

The study was undertaken after obtaining the approval of institutional ethical committee clearance for excisional and incisional wound healing (registration number: XVI/VELS/PCOL/08/2000/CPCSEA/IAEC/25.11.14) and diabetic-induced excisional and incisional wound healing (registration number: XVII/VELS/PCOL/06/2000/CPCSEA/IAEC/06.10.15).

2.9.2 | Experimental animals

Healthy, adult Wistar albino rats of both genders weighing 150–200 g were used for the experiment. They were inbred in the Vels University animal house. Animals were individually housed and maintained under standard conditions at $25 \pm 2^\circ\text{C}$, relative humidity of 50 to 60% and 12:12 hours light and dark cycles, and they were allowed free access to a standard pellet diet and water ad libitum. The animals were housed for 1 week prior to the experiments to be acclimatised to laboratory conditions.

2.9.3 | Ointment formulation

Cb-peptide was formulated to an ointment²⁰; an ointment with a water-soluble base was the first choice because of its easy preparation and cleaning after application. Polyethylene glycol (PEG) ointment based on a mixture of PEG 4000 and PEG 600 was found to have sufficient consistency in a ratio of 3:7, thus suitable for ointment preparation with a concentration of Cb-peptide of 1 mg/mL for a high dose and 0.5 mg/mL for a low dose.

2.9.4 | Excision wound model

Four groups of healthy, adult Wistar albino rats of either gender weighing 150–200 g, with 6 animals (3 males and 3 females) in each group, were anaesthetised by anaesthetic ether in desiccators. The rats were depilated on their backs, and cutaneous circular wounds of 8 mm diameter were inflicted on the pre-shaved sterile dorsal surface of the animal by cutting; in each group, each animal received 1 wound.²¹ Animals were housed individually in metallic cages. The wound was left undressed to the open

environment. Then, the treatment was started in the following manner:

Group I: vehicle control (ointment base without Cb-peptide)

Group II: standard control (povidone iodine 5% w/w ointment)

Group III: Cb-peptide ointment (low dose 0.5 mg/mL)

Group IV: Cb-peptide ointment (high dose 1 mg/mL).

The drug was applied once a day after cleaning the wound with surgical cotton wool.

The percentage of wound contraction was calculated by using the formula:

$$\text{Percentage of wound contraction} = \frac{\text{Healed area}}{\text{Total wound area}} \times 100$$

2.9.5 | Incision wound model

Four groups of rats containing 3 animals in each group were anaesthetised, and 1 paravertebral long incision was made through the skin and cutaneous muscle at a distance of about 1.5 cm from the midline on each side of the depilated back of the Wistar albino rat.²²

After the incision was made, the parted skin was held together and stitched with black silk at 0.5 cm intervals; surgical thread (no. 000) and curved needle (no. 11) were used for stitching. The continuous thread on both wound edges was tightened for good closure of the wound.²³ The wound was left undressed. Then, the treatment was started in the same manner as mentioned in the case of excision wound model:

Group I: vehicle control (ointment base without Cb-peptide)

Group II: standard control (povidone iodine 5% w/w ointment)

Group III: Cb-peptide ointment (low dose 0.5 mg/mL)

Group IV: Cb-peptide ointment (high dose 1 mg/mL).

The drug was applied once a day after cleaning the wound with surgical cotton wool. All the ointment was applied for 9 days to their respective groups. When wounds were cured thoroughly, the sutures were removed on the ninth day, and tensile strength was measured using a tensiometer.^{24,25}

2.9.6 | Induction of diabetes in Wistar albino rats

All the rats were fasted overnight before the administration of alloxan. Diabetes mellitus was induced by a single intraperitoneal injection of freshly prepared alloxan monohydrate (alloxan monohydrate dissolved in 0.9% w/v normal saline solution) (120 mg/kg) according to body weight.²⁶ Diabetes was developed and stabilised in the alloxan-treated rats over a period of 3 days. After 3 days of alloxan administration, the blood sugar level of each rat was determined. A range of more than 200 mg/dL was considered diabetic and included in this study.²⁷ Blood was collected from the tail vein after induction of diabetes excision and incision wounds were created in the diabetic-induced Wistar albino rats.

2.10 | Histopathological examination

After day 21, the experiment was terminated and the animals were selected randomly. The wound area from the surviving animal was removed just beneath the epidermis or at deep dermis for histological examination. At the insisted area, in every skin section area just beneath the epidermis and also deep dermis randomly selected. Granulation tissues were fixed in 10% neutral formalin solution for 24 hours and dehydrated with a sequence of ethanol-xylene series of solutions.²⁸ The materials were filtered and embedded with paraffin (40-60°C). Microtome sections were taken at a thickness of 10 µm. The sections were processed in alcohol-xylene series and stained with haematoxylin-eosin dye. The histological changes were observed under a microscope. The different animal groups were assessed by the pathologist, and results were compared with the control and standard groups.

2.11 | Statistical analysis

Statistical comparison was performed using 1-way analysis of variance (ANOVA), and comparisons vs control group was performed by Dunnett's test. All statistical analysis was performed using SPSS statistical version 16.0 software; *P* values <0.05 were considered statistically significant.

3 | RESULTS

3.1 | Purification and identification of antimicrobial peptide

After papain enzyme digestion, the protein hydrolysate of *C. bistrialis* was separated into 2 fractions based on molecular weight—low (<10 kDa) and high (>10 kDa); both were screened against antimicrobial activity. Activity-rich high (>10 kDa) fraction was further applied onto a RP-HPLC C-18 column; 60 different fractions were collected, and the antimicrobial activities of all fractions were evaluated. Activity-rich fractions were pooled together and were analysed using the MALDI-TOF/TOF; higher-activity fractions consisted of a single peptide that exhibited an *m/z* value of 21.79 kDa (Figure 1A,B).

3.2 | Partial sequence of the Cb-peptide Masscot search

Protein sequence coverage: 53%.

Matched peptides shown in *bold red*.

1	PWRSISEIHQ	PHNILQRRLM	ETNLSKLRSS	RVPWASKTNK	LNQAKSEGLK
51	KSEDDDMILV	SCQCAGK DVK	ALVDTGCQYN	LISSACVDRL	GLKEHVRSHK
101	HEGKLSLPR	HLKVVQGIEH	LVITLGLSLRL	DCPAAVVEDN	EKNLSLGLQT
151	LRLSKCIINL	DKHRLIMGKT	DKEEIPFVET	VSLNEDNTSE	A

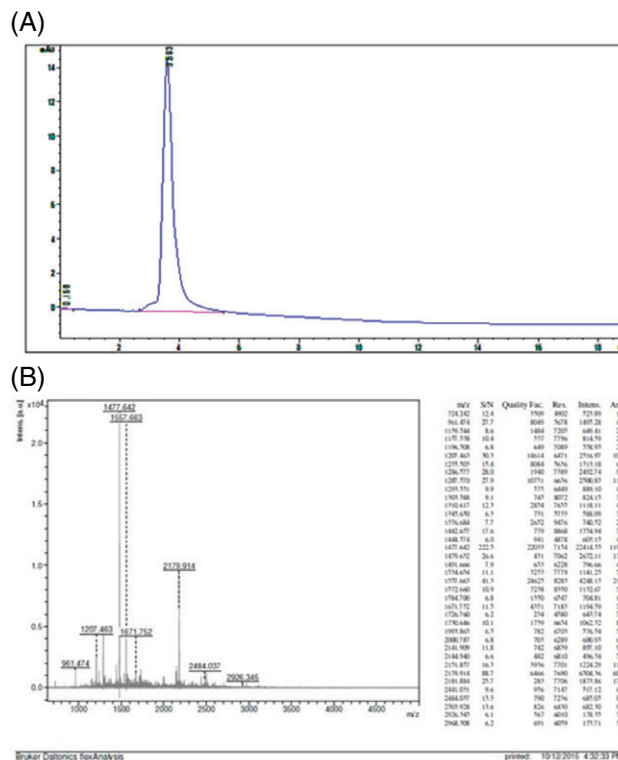


FIGURE 1 (A) Reversed-phase high-performance liquid chromatography and (B) spectrum of MALDI-TOF

3.3 | Characterisation of Cb-peptide using various analytical methods

UV-visible, fluorescence and CD spectroscopy of the Cb-peptide were carried out. Figure 2A shows the UV-visible spectra of the Cb-peptide. A broad shoulder peak around 280 nm clearly shows the presence of Trp in the Cb-peptide. Figure 2B shows the steady-state fluorescence measurements of the Cb-peptide, and it can be seen that the Trp emission is at 340 nm. More work is underway to crystallise the Cb-peptide and identify the sequence, which will enhance our knowledge of the structure of the peptide. CD spectra of the Cb-peptide (Figure 2C) show a mix of helical and beta turn conformations. When fitted using DICHROWEB, the values were α -helix, 16%; β -sheet, 8.1%; β -turn, 31.2%; and random coil, 39.7%. For a better anti-diabetic property of the peptide, uniform self-assembly is essential.^{29,30} Figure 2D shows SEM images of the Cb-peptide with a uniform self-assembly, and thus, the Cb-peptide can be used for anti-diabetic treatment.

3.4 | Antimicrobial activity of the peptide from *C. bistrialis*

Antibacterial and antifungal activity of the Cb-peptide was evaluated and is presented in Tables 1 and 2.

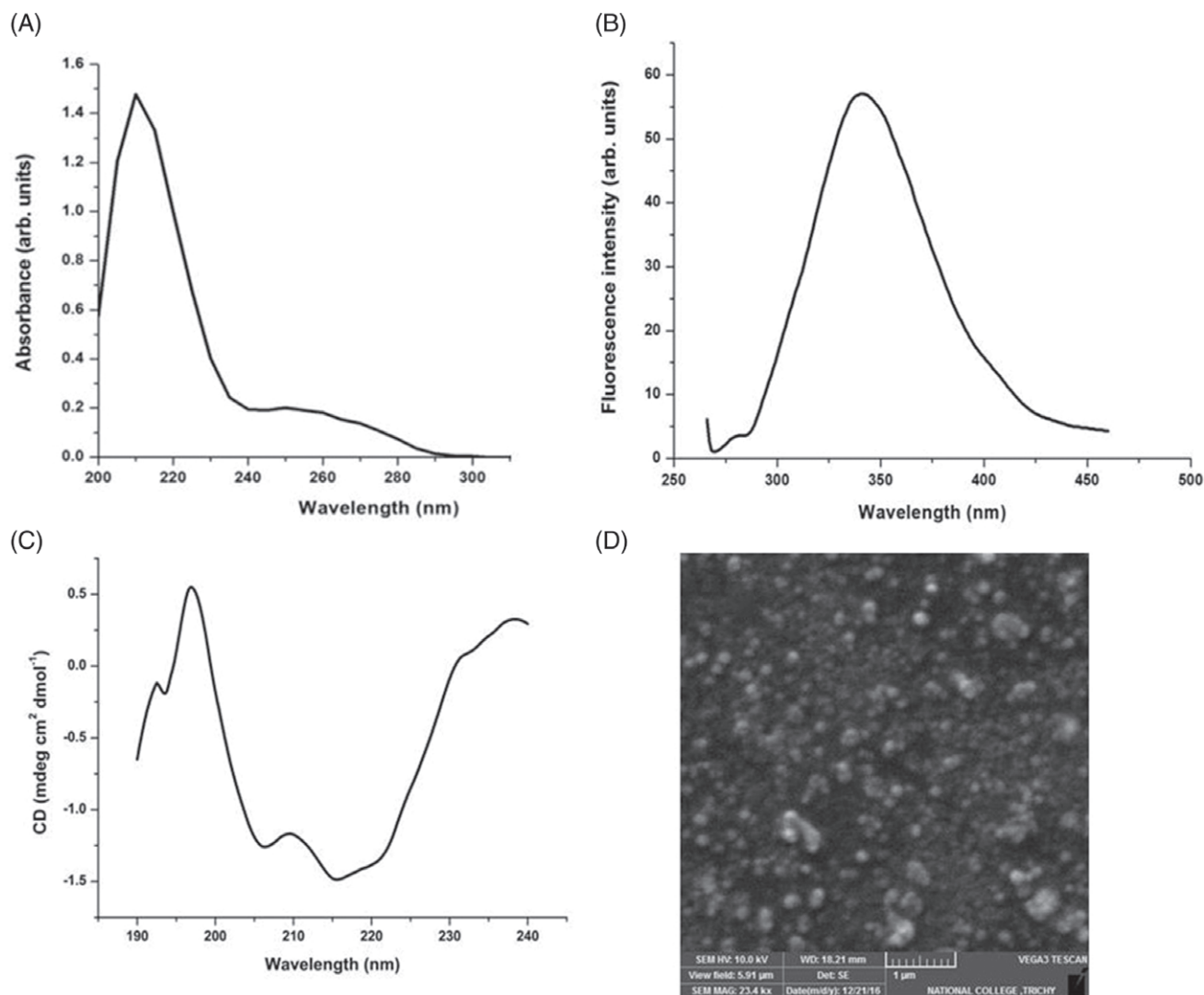


FIGURE 2 (A) UV-Vis spectra; (B) fluorescence spectra; (C) circular dichroism spectra; and (D) Scanning electron microscopy image of the peptide

TABLE 1 Minimum inhibitory concentration of the Cb-peptide against bacterial cultures

Organisms	Minimum inhibitory concentration ($\mu\text{g/mL}$)					
	<i>Pseudomonas aeruginosa</i>	<i>Proteus vulgaris</i>	<i>Hafnia alvei</i>	<i>Serratia marcescens</i>	<i>Staphylococcus aureus</i>	<i>Micrococcus luteus</i>
Cb-peptide	3.12 ^a (93.2 ^b)	6.2 ^a (90.1 ^b)	6.25 ^a (86.13 ^b)	3.1 ^a (90.9 ^b)	3.12 ^a (89.8 ^b)	6.25 ^a (85.9 ^b)

^a Cb-peptide concentration ($\mu\text{g/mL}$) that inhibits the bacteria.

^b LC₅₀ values are expressed as the concentration that causes 50% decrease in optical density of microorganism suspension.

3.5 | In vitro assay for cytotoxicity activity of peptide from *C. bistrialis* (MTT assay)

MTT assay was performed for the Cb-peptide to find the cytotoxic effect on NIH/3T3 mouse fibroblast cells. Results are presented in Figure 3.

TABLE 2 Minimum inhibitory concentration of the Cb-peptide against fungal cultures

Organisms	Minimum inhibitory concentration ($\mu\text{g/mL}$)			
	<i>Candida albicans</i>	<i>Penicillium chrysogenum</i>	<i>Aspergillus fumigatus</i>	<i>Mucor racemosus</i>
Cb-peptide	25 ^a (85.4 ^b)	50 ^a (82.1 ^b)	50 ^a (82.1 ^b)	12.5 (84.9)

^a Cb-peptide concentration ($\mu\text{g/mL}$) that inhibits the microbial growth.

^b LC₅₀ values are expressed as the concentration that causes 50% decrease in optical density of microorganism suspension.

Based on the MTT results, a 50 $\mu\text{g/mL}$ concentration of Cb-peptide was selected for in vitro wound-healing activity.

3.6 | In vitro wound scratch assay of Cb-peptide

Wound scratch assay was performed in NIH/3T3 mouse fibroblast cell line. Wound-healing activity of the Cb-peptide was tested at different time intervals, presented in Figure 4.

Cb-peptide was tested at different time intervals using the scratch assay method to determine the migration of fibroblast cells. Control cells are not closed in the scratched area. Cb-peptide-treated NIH/3T3 cells were found to migrate faster following the 18th hour of the

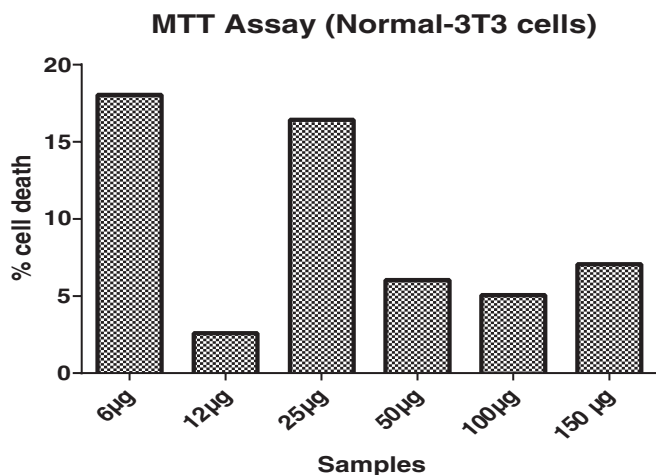


FIGURE 3 MTT assay of Cb-peptide

incubation period; full wound healing was observed in the 48th hour of incubation. The results demonstrated that the Cb-peptide administration created a difference in wound closure rate between the treated and control groups. It was also noticed that NIH/3T3 cells migrated rapidly to fill the wounded area.

3.7 | In vivo wound-healing activity of Cb-peptide

Wound-healing activity of Cb-peptide was evaluated in Wistar albino rats, and the results are presented in Figure 5A-D, Tables 3 and 4.

Two different wound models were used to analyse the wound-healing potential of Cb-peptide in 2 different concentrations, low dose (0.5 mg/mL) and high dose (1 mg/mL). Cb-peptide was evaluated in a normal excision and incision wound model and a diabetic-induced excision and incision wound model in Wistar albino rats. Thus, in this study, wound closure rates, percentage of wound contraction, epithelialisation period and tensile strength were

studied. Wound-healing activity of the Cb-peptide was evaluated in diabetic-induced Wistar albino rats. Wound-healing parameters were noted on different days, and the results are presented in Figure 6A-D, Tables 5 and 6.

3.8 | Histopathology analysis

After the 21st day, the experiment was terminated. Tissue was removed from the wound's healed area, and microtome sections were taken and stained with haematoxylin-eosin dye. The histological changes were observed under a microscope (Figures 7–10).

The Cb-peptide ointment-treated rats showed marked epithelialisation, a moderate amount of extracellular matrix synthesis, and new blood vessel formation. Histopathological examination demonstrated that tissue regeneration was much quicker in the Cb-peptide ointment-treated group compared with the vehicle control group and standard ointment-treated group.

4 | DISCUSSION

Impaired wound healing continues to be a major health problem that predisposes to infections, long-term morbidity, and mortality, particularly in high-risk patients who may consequently suffer from diabetic skin ulcer and even amputation.^{31–33} Therefore, developing new drugs and treatment methods will be eagerly expected. In this study, Cb-peptide was demonstrated to contain excellent antimicrobial and wound-healing properties in normal and diabetic-induced Wistar albino rats.

Guerard et al³⁴, Sathivel et al³⁵, and Kong et al³⁶ explained the enzyme digestion method in their work, and they were used tuna waste by protease enzyme. Booncharoen and Thammasirirak³⁷ researched the antimicrobial peptide released by enzymatic hydrolysis of a soft-shelled turtle

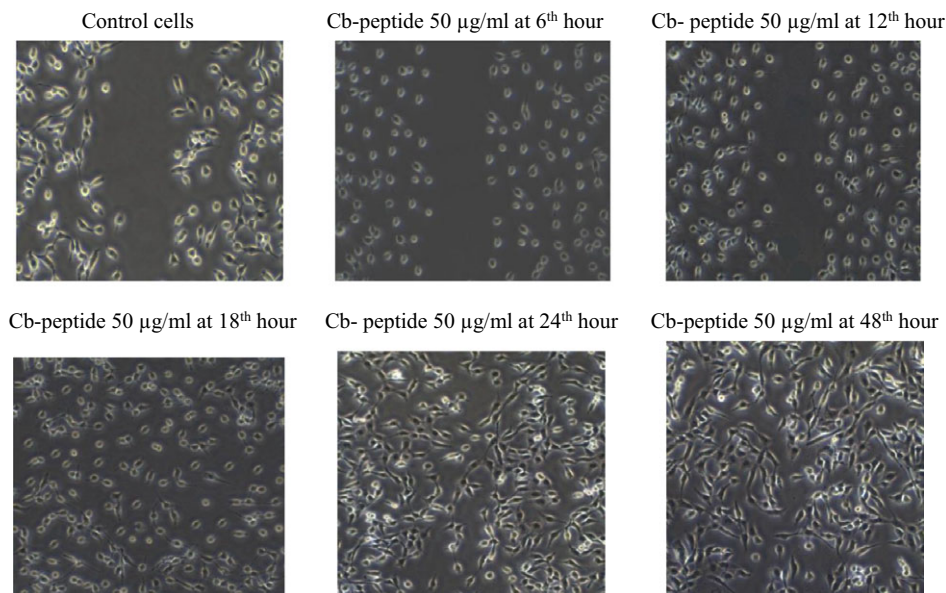


FIGURE 4 In vitro wound scratch assay of Cb-peptide

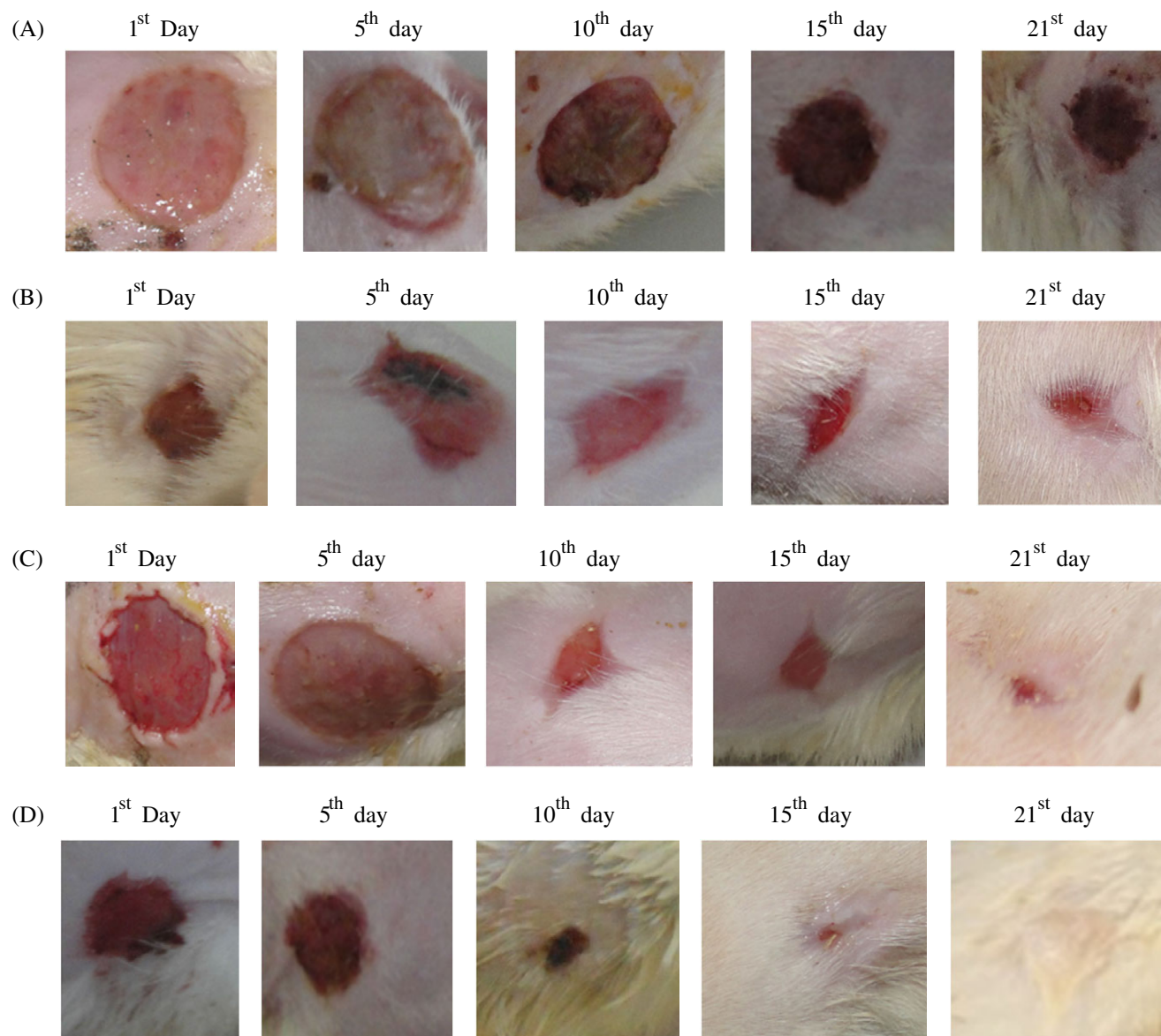


FIGURE 5 (A). Group I: vehicle control (ointment base) (magnified wound contraction view of vehicle control treated excision wound model of Wistar albino rats on different days); (B) Group II: standard control (povidone iodine 5% w/w ointment) (magnified wound contraction view of standard control treated excision wound model of Wistar albino rats on different days); (C) Group III: Cb-peptide ointment (low dose 0.5 mg/mL) (magnified wound contraction view of Cb-peptide ointment (low dose 0.5 mg/mL)-treated excision wound model of Wistar albino rats on different days); (D) Cb-peptide ointment (high dose 1 mg/mL) (magnified wound contraction view of Cb-peptide ointment (high dose 1 mg/mL)-treated excision wound model of Wistar albino rats on different days)

lysozyme. In the present study, the papain enzyme was used to release peptide from *C. bistrialis*. Adikwu and Alozie³⁸ purified and characterised 8 peptides from *Galleria mellonella*, differing in their molecular weight, which were

analysed using the MALDI-TOF, and antimicrobial assays were also performed for the purified 8 peptides. Lopez-Abarrategui et al³⁹ isolated and characterised synthetic hydrophilic antifungal peptide derived from the marine snail

TABLE 3 Excision wound-healing activity of Cb-peptide

Groups	Wound contraction (mm) ²					Period of epithelialisation
	Day 0	Day 5	Day 10	Day 15	Day 21	
Vehicle control	110.24 ± 6.5 (0.00)	94.16 ± 2.85 (14.54)	81.83 ± 3.37 (26.36)	63 ± 3.34 (37)	29 ± 3.34 (73.63)	27.1 ± 0.30
Standard control	109.5 ± 6.15 (0.00)	69.89 ± 3.43 _a (36.69)	21.66 ± 2.87 _b (80.7)	3.5 ± 0.54 _c (97.2)	0.00 (100)	18.16 ± 0.4
Cb-peptide high dose	110.26 ± 7.1 (0.00)	54.66 ± 3.77 _a (50.90)	12 ± 1.26 _c (89.09)	0.00 (100)	0.00 (100)	13.3 ± 0.2
Cb-peptide low dose	110.55 ± 5.7 (0.00)	60.5 ± 2.42 _b (45.4)	17.53 ± 1.96 _c (94.54)	5.66 ± 1.63 _c (105.45)	0.00 (100)	17.0 ± 0.42

Values are expressed as mean ± SEM, $n = 6$; 1-way ANOVA followed by Dunnett's t -test; t -values denote significance at (a) $P < .05$, (b) $P < .1$, (c) $P < .001$. Percentage of wound contraction presented in parenthesis.

TABLE 4 Breaking strength of incision wound healing on the 10th post-wounding day

Groups	Breaking strength (g)
Vehicle control	306.33 ± 27.8
Standard control	413.66 ± 16.36
Cb-peptide low dose	420.66 ± 29.85
Cb-peptide high dose	550.66 ± 21.08

Wound-breaking strength of various ointment-treated groups. The data were expressed as a mean of triplicates ± SD.

Cenchrithis muricatus. The peptide was analysed by MALDI-TOF, and mass value of the peptide was 14.85 kDa. Cb-peptide was purified by RP-HPLC, and molecular weight was analysed using the MALDI-TOF method; mass value was 21.79 kDa, illustrated in Figure 1A,B.

The Cb-peptide exhibits a broad spectrum of antimicrobial activity against the Gram-positive bacteria *S. aureus* and Gram-negative bacteria *P. aeruginosa* and the fungal species *C. albicans* and *M. racemosus*.

Adolphe et al⁴⁰, Bucalo et al⁴¹, and Park et al⁴² reported in their in vitro studies that fibroblast proliferation had been adopted as an indicator for the assessment of wound healing. Fibroblast was the major cell type found in the granulation of wound tissues. Mansbridge et al⁴³ stated that fibroblasts play an essential role in wound healing, including secretion of a series of growth factors that facilitates angiogenesis, proliferation, and matrix deposition. In our current work, in vitro studies of the fibroblast NIH/3T3 were used to analyse its wound-healing activity; the Cb-peptide significantly enhanced fibroblast cell proliferation and indicated increased response in migration in wound scratch assay.

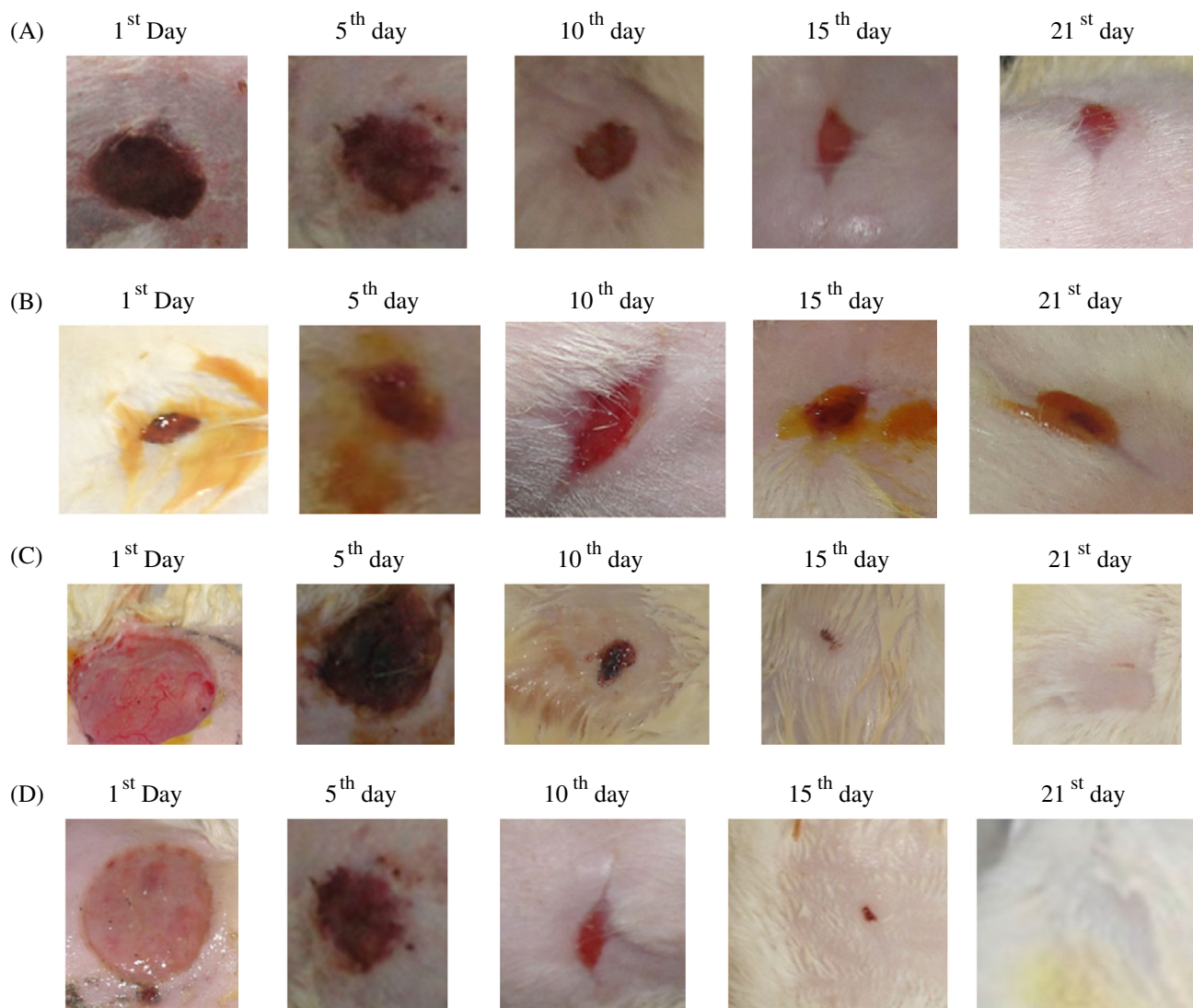


FIGURE 6 (A) Group I: vehicle control (ointment base) (magnified wound contraction view of vehicle control treated diabetic-induced excision wound model of Wistar albino rats on different days); (B) Group II: standard control (magnified wound contraction view of standard control treated diabetic-induced excision wound model of Wistar albino rats on different days); (C) Group 3: Cb-peptide low dose (0.5 mg/mL) (magnified wound contraction view of Cb-peptide ointment low dose (0.5 mg/mL) treated diabetic-induced excision wound model of Wistar albino rats on different days); (D) Group IV: Cb-peptide high dose (1 mg/mL) (magnified wound contraction view of Cb-peptide ointment high dose (1 mg/mL) treated diabetic-induced excision wound model of Wistar albino rats on different days)

TABLE 5 Diabetic-induced excision wound-healing activity of Cb-peptide

Groups	Wound contraction (mm) ²					Period of epithelisation
	Day 0	Day 5	Day 10	Day 15	Day 21	
Vehicle control	86.3 ± 3.1 (0.00)	80.16 ± 2.70 (6.97)	56.1 ± 3.40 (34.88)	50.1 ± 2.14 (41.86)	25.27 ± 2.66 (70.93)	30.24 ± 0.36
Standard control	85.5 ± 6.5 (0.00)	52.1 ± 3.17b (38.82)	14.1 ± 2.05c (83.52)	0.00 (100)	0.00 (100)	14.18 ± 0.3
Cb-peptide high dose	85 ± 3.8 (0.00)	47.1 ± 4.43a (44.70)	3.66 ± 2.3c (96.47)	0.00 (100)	0.00 (100)	12 ± 0.2
Cb-peptide low dose	86.5 ± 2.8 (0.00)	50.66 ± 1.62c (41.86)	10.5 ± 0.5c (88.37)	0.00 (100)	0.00 (100)	13.50 ± 0.4

Values are expressed as mean ± SEM, $n = 6$; 1-way ANOVA followed by Dunnett's *t*-test; *t*-values denotes significance at (a) $P < .05$; (b) $P < .1$; (c) $P < .001$. Percentage of wound contraction presented in parenthesis.

TABLE 6 Breaking strength of diabetic-induced incision wound healing on the 10th post-wounding day

Groups	Breaking strength (g) Diabetic
Vehicle control	316.0 ± 25
Standard control	491.66 ± 15.36c
Cb-peptide high dose	596.66 ± 33.4c
Cb-peptide low dose	440.66 ± 17.25b

Breaking strength of various ointment-treated groups. Values are expressed as a mean of triplicates ±SD.

In the present study, the Cb-peptide showed significant cellular activities, such as maximum collagen deposition, regeneration of blood vessels, and significant epithelialization, in the diabetic-induced excision wound model; this proves the wound-healing capability of Cb-peptide.

In the diabetic-induced excision wound model, the Cb-peptide ointment-treated group exhibited faster wound contraction and re-epithelialisation. The percentage of wound closure was also higher in Cb-peptide ointment-treated Wistar albino rats. Raghov⁴⁴ reported that collagen provides strength and integrity to the repaired dermis. In our present study, the diabetic-induced incision wound model showed an increased amount of tensile strength in Cb-peptide ointment-treated group compared with vehicle control and standard control treated groups due to the increase in collagen concentration and stabilisation of fibres; this indicate it has a wound-healing property.

Smith et al⁴⁵ and Flanagan⁴⁶ stated that wound size measurement has long been used to assess the progress of wound healing. In the present work, in the excision wound model, the Cb-peptide high dose (1 mg/mL) ointment showed significant increase in the percentage of wound closed by enhanced epithelialisation. This higher percentage of wound healing may be due to the effect of the Cb-peptide on enhanced collagen synthesis, which was verified using histopathological studies. The increased wound contraction in the test group may be due to the Cb-peptide. A significant increase in collagen content due to enhanced migration of fibroblasts and epithelial cells to the wound site was observed during the wound-healing process in the Cb-peptide ointment-treated group.

A close examination of granulation tissue sections showed that tissue regeneration was much quicker in the Cb-peptide ointment-treated group compared with that in the vehicle control and standard control treated wound. Early dermal and epidermal regeneration in the treated group confirmed that the ointment containing Cb-peptide

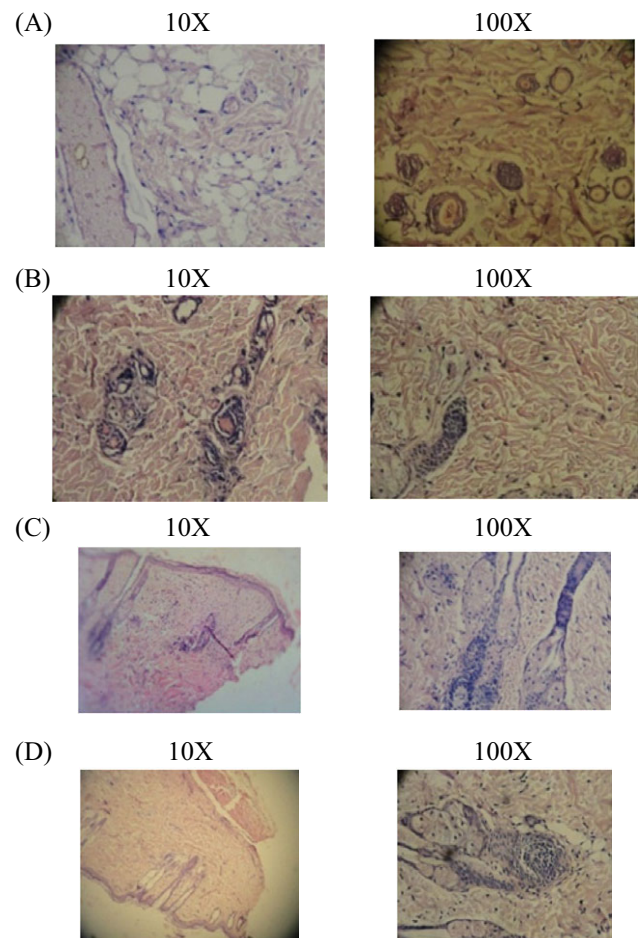


FIGURE 7 (A–D) Histopathology study of excision wound healing. In the excision wound model, 4 groups are present, the results of histopathological changes are presented. (A) Group I: vehicle control (ointment base)—collagen not fully formed, scanty granulation tissue with minimum fibroblast; (B) Group II: standard control—better granulation tissue formation and collagenisation with fibroblast; (C) Group III: Cb-peptide ointment (low dose)—greater degree of granulation tissue formation and collagenisation with fibroblast; (D) Group IV: Cb-peptide ointment (high dose)—maximum collagenisation, epithelialisation was early and complete

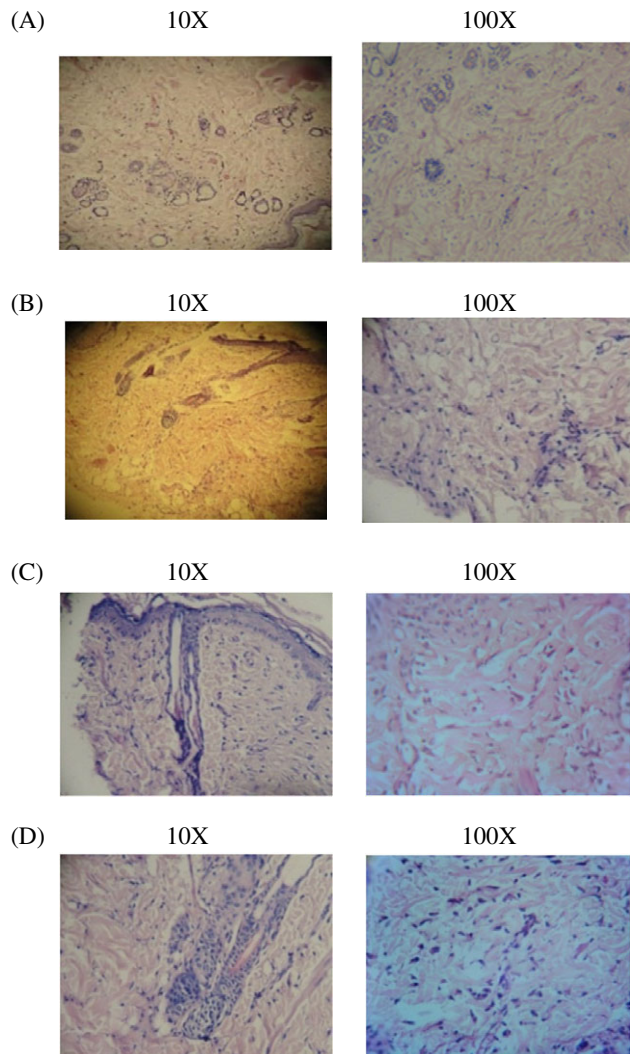


FIGURE 8 (A-D) Histopathology study of incision wound healing. In the incision wound model, 4 groups are present; the results of histopathological changes are presented. (A) Group I: vehicle control—collagen fibres not fully formed and minimum fibroblast; (B) Group II: standard control—minimum collagenisation scattered and mixed inflammatory cells; (C) Group III: Cb-peptide low dose—healed ulcer, fibrosis and epithelisation. Maximum collagen fibres and fibroblast; (D) Group IV: Cb-peptide high dose—maximum collagen deposition, greater degree of fibroblast proliferation

had a positive effect on cellular proliferation, granulation tissue formation, and epithelialisation. Incomplete epithelialisation with less extracellular matrix synthesis was observed in vehicle control treated Wistar albino rats. In the incision wound model, greater breaking strength was observed in Cb-peptide ointment-treated rats compared with standard control and vehicle control treated rats.

5 | CONCLUSION

Current treatments for diabetic wounds fail to achieve effective therapeutic outcomes. A good sign of regenerative wound healing is rapid and effective re-epithelialisation.

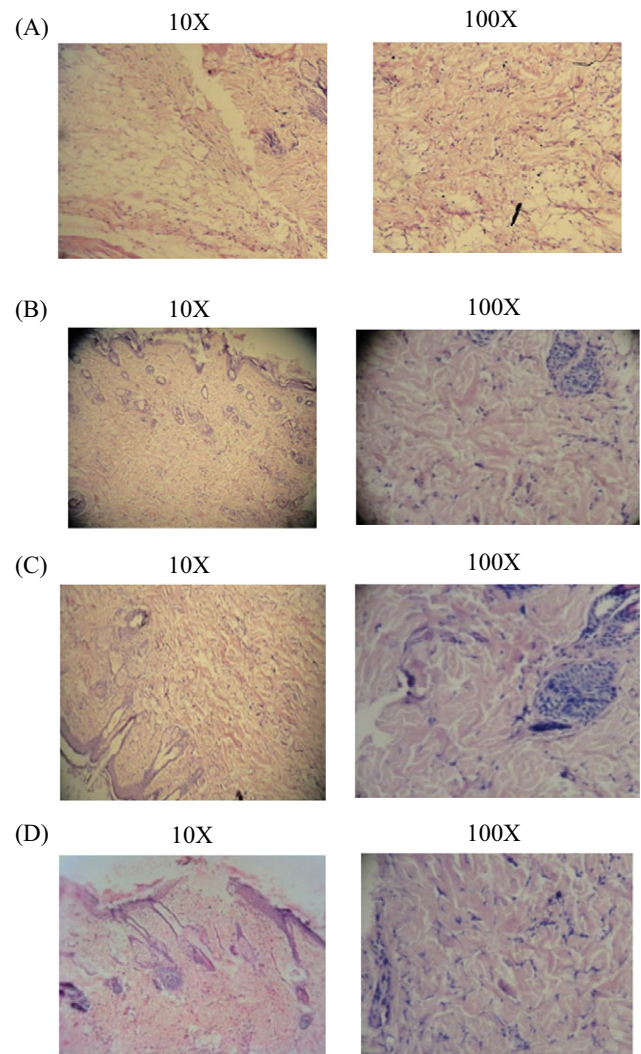


FIGURE 9 (A-D) Histopathology study of diabetic-induced excision wound healing. In the excision wound model, 4 groups are present; the results of histopathological changes are presented. (A) Group I: vehicle control—ulcer covered by debris; oedema; congested vessels; and scattered, mixed inflammatory cells; (B) Group II: standard control—maximum collagenisation and scattered inflammatory cells; (C) Group III: Cb-peptide ointment (low dose)—healed ulcer, maximum collagen deposition; no inflammatory cell collection or granuloma is detected; (D) Group IV: Cb-peptide ointment (high dose)—maximum collagen fibres formed, fully healed ulcer without any oedema

Microbial infection is the major factor that affects the healing process of the wound. In this study, the peptide derived from the terrestrial snail *C. bistrialis* proved the antimicrobial activity against pathogenic bacterial and fungal cultures and demonstrates that it can be a therapeutic candidate that targets re-epithelialisation. The Cb-peptide promoted cell migration of NIH/3T3 mouse fibroblast cells in vitro. In vivo studies demonstrated that the Cb-peptide was effective in promoting wound healing in normal and diabetic-induced Wistar albino rats. Further investigations intending to crystallise the Cb-peptide and identify the sequence are required, which will enhance our knowledge on the structure of the peptide.

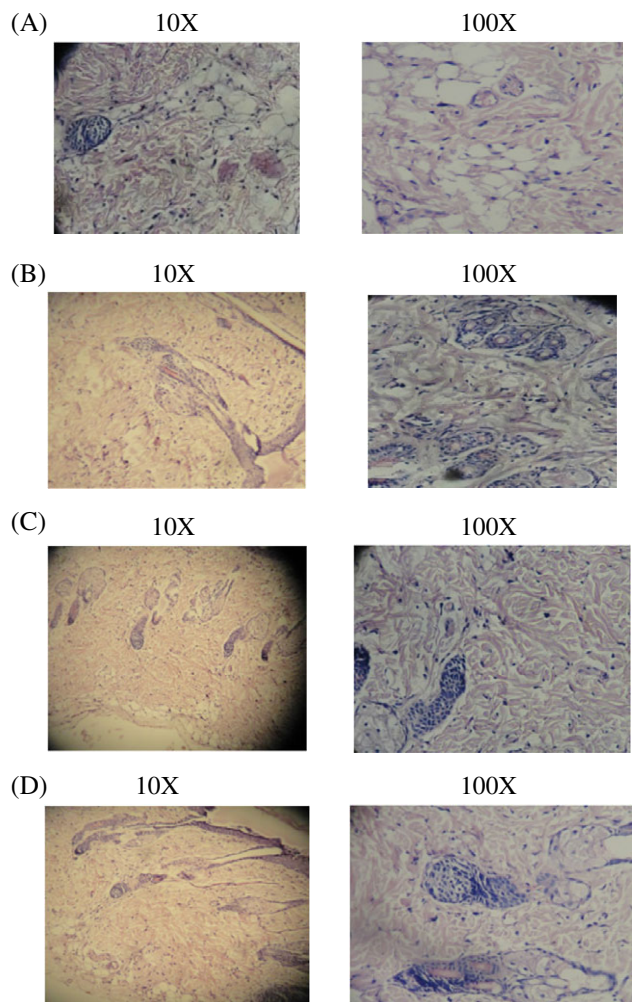


FIGURE 10 (A–D) Histopathology study of diabetic-induced incision wound healing. In the incision wound model, 4 groups are present; the results of histopathological changes are presented. (A) Group I: vehicle control—abundant granulation with scanty collagen tissues; (B) Group II: standard control—better collagen deposition and scattered inflammatory cells; (C) Group III: Cb-peptide ointment low dose—maximum collagen deposition and fibroblast proliferation; (D) Group IV: Cb-peptide high dose—maximum granulation tissue formation and greater degree of collagen deposition

ACKNOWLEDGEMENTS

The Corresponding author US thanks Mr. V.Santhosh Kumar, Head of the Department and Mrs. Manjula Devi, Assistant Professor, School of Pharmaceutical Sciences, Department of Pharmacy, Vels University, Tamil Nadu, India. One of the authors, KS thanks Department of Science and Technology, Govt. of India for the INSPIRE Faculty Award (Dy. No. 108 Dt. 8.1.2014).

REFERENCES

1. Tam JCW, Lau KM, Liu CL, et al. The *in vivo* and *in vitro* diabetic wound healing effects of a 2-herb formula and its mechanisms of action. *J Ethnopharmacol.* 2011;134:831–838.
2. Adikwu MU, Alozie BU. Application of snail mucin dispersed in detarium gum gel in wound healing. *Sci Res Essay.* 2007;2:195–198.
3. Brownlee M. Glycation products and the pathogenesis of diabetic complications. *Diabetes Care.* 1992;15:1835–1843.

4. Clark RA. Fibrin and wound healing. *Ann N Y Acad Sci.* 2001;936:355–367.
5. Nayak BS, Marshall MR, Isitor G. Wound healing potential of ethanolic extract of *Kalanchoe pinnata* lam. Leaf-a preliminary study. *Indian J Exp Biol.* 2010;48:572–576.
6. Wang N, Liang H, Zen K. Molecular mechanisms that influence the macrophage M1-M2 polarization balance. *Front Immunol.* 2014;5:614.
7. Blunt JW, Copp BR, Munro MHG, Northcote PT, Prinsep MR. Marine natural products. *Nat Prod Rep.* 2006;26:170–244.
8. Anand PT, Edward JKP. Antimicrobial activity in the tissue extracts of five species of cowries *Cypraea* sp. (Mollusca: gastropoda) and an ascidian *Didemnum psammathodes* (Tunicata:Didemniidae). *Ind J Mar Sci.* 2002;25:239–242.
9. Kamiya H, Muramoto K, Goto R, Sakai M, Endo Y, Yamazaki M. Purification and characterization of an antibacterial and antineoplastic protein secretion of a sea hare, *Aplysia juliana*. *Toxicon.* 1989;27:1269–1277.
10. Pettit GR, Kamano Y, Herald CI. The isolation and structure of a remarkable marine animal antineoplastic constituent, dolastatin-10. *J Am Chem Soc.* 1987;109:6883–6885.
11. Kisugi J, Ohye H, Kamiya H, Yamazaki M. Biopolymers from marine invertebrates. Mode of action of antibacterial glycoprotein Aplysianin E, from eggs of a sea hare, *Aplysia kurodai*. *Chem Pharm Bull.* 1989;37:2773–2776.
12. Rajaganapathi J, Thiyagarajan SP, Edward JKP. Study on Cephalopods ink for antiviral activity. *Indian J Exp Biol.* 2000;38:519–520.
13. Gonzalez Y, Tanaka AS, Hirata IY, et al. Purification and partial characterization of human neutrophil elastase inhibitors from the marine snail *Cenchritis muricatus* (Mollusca). *Comp Biochem Physiol A Mol Integr Physiol.* 2007;146:506–513.
14. Quave CL, Pieroni A, Bennett BC. Dermatological remedies in the traditional pharmacopoeia of Vulture-Alto Brandano, inland southern Italy. *J Ethnobiol Ethnomed.* 2008;4:5.
15. Nnanna IA, Wu C. Dairy protein hydrolysates. In: Hui YH, ed. *Handbook of Food Products Manufacturing.* Vol 2. India: John Wiley & Sons, Inc.; 2007:537–556.
16. Je JY, Qian Z, Byun HG, Kim SK. Purification and characterization of an antioxidant peptide obtained from tuna backbone protein by enzymatic hydrolysis. *Process Biochem.* 2007;42:846–849.
17. Lauth X, Shike H, Burns JC, et al. Discovery and characterization of two isoforms of moronecidin, a novel antimicrobial peptide from hybrid striped bass. *J Biol Chem.* 2002;277:5030–5039.
18. Mosmann T. Rapid colorimetric assay for cellular growth and survival: application to proliferation and cytotoxicity assays. *J Immunol Methods.* 1983;65:55–63.
19. Liang CC, Park AY, Guan JL. *In vitro* scratch assay: a convenient and inexpensive method for analysis of cell migration *in vitro*. *Nat Protoc.* 2007;2:329–333.
20. Bupesh G, Subramanian P. Wound healing activity of PL-peptide on albino rats. In: Subramanian P, ed. *An Anthology of Articles on Aquat Research.* India: Nitheesh Prabha Pathippagam; 2011:133–144.
21. Boominathan R, Parimaladevi B, Mandal SC, Ghosal SK. Anti-inflammatory evaluation of ionidium suffruticosam ging in rats. *J Ethnopharmacol.* 2004;91:367–370.
22. Khan MA, Saxena A, Fatima FT, Sharma G, Goud V, Husain A. Study of wound healing activity of *Delonix regia* flowers in experimental animal models. *Am J Pharm Tech Res.* 2012;2:380–390.
23. Dewangan H, Bais M, Jaiswal V, Verma VK. Potential of wound healing activity of ethanolic extract of *Solanum xanthocarpum* schrad and wendl leaves. *Pak J Pharm Sci.* 2012;25:189–194.
24. Zahra AA, Kadir FA, Mahmood AA, et al. Acute toxicity study and wound healing potential of *Gynura procumbens* leaf extract in rats. *J Med Plants Res.* 2011;5:2551–2558.
25. Lee KH. Studies on the mechanism of action of salicylate II. Retardation of wound healing by aspirin. *J Pharm Sci.* 1968;57:1042–1043.
26. Cooper Stein SJ, Walkin D. The Islets of Langer. New York: Academic Press; 1981:387–425.
27. Santoni G, Perfumi M, Bressan AM, Piccoli M. Capsaicin-induced inhibition of mitogen and interleukin-2-stimulated T cell proliferation: its reversal by *in vivo* substance P administration. *J Neuroimmunol.* 1996;68:131–138.
28. Mukherjee KL. Medical Laboratory Technology, a Procedure Manual for Routine Diagnostic Tests I. New Delhi, India: Tata McGraw Hill Publishers; 2000.

29. Koria P, Yagi H, Kitagawa Y, et al. Self-assembling elastin-like peptides growth factor chimeric nanoparticles for the treatment of chronic wounds. *Proc Natl Acad Sci U S A*. 2011;108:1034-1039.
30. Castleberry SA, Almquist BD, Li W, et al. Self-assembled wound dressings silence MMP-9 and improve diabetic wound healing *in vivo*. *Adv Mater*. 2016;28:1809-1817.
31. Nathan BM, Kevin RW, Tarynn MW, Danaïl GB, Robert FD. Impaired wound healing. *Clin Dermatol*. 2007;25:19-25.
32. Nwomeh BC, Yager DR, Cohen IK. Physiology of the chronic wound. *Clin Plast Surg*. 1998;25:341-356.
33. Brem H, Balledux J, Bloom T. Healing of diabetic foot ulcers and pressure ulcers with human skin equivalents. *Arch Surg*. 2000;135:627-634.
34. Guerard F, Guimas L, Binet A. Production of tuna waste hydrolysates by a commercial neutral protease preparation. *J Mol Catal B: Enzym*. 2002;19:489-498.
35. Sathivel S, Bechtel PJ, Babbitt J, Smiley S, Crapo C, Reppond KD. Biochemical and functional properties of herring (*Clupea harengus*) by product hydrolysates. *J Food Sci*. 2003;68:2196-2200.
36. Kong X, Zhou H, Qian H. Enzymatic hydrolysis of wheat gluten by proteases and properties of the resulting hydrolysates. *Food Chem*. 2007;102:759-763.
37. Booncharoen S, Thammasirirak S. Antimicrobial peptide released by enzymatic hydrolysis of soft shelled turtle lysozyme. *KMITL Sci Tech J*. 2007;7:1.
38. Adikwu MU, Alozie BU. Application of snail mucin dispersed in detarium gum gel in wound healing. *Sci Res Essay*. 2007;2:195-198.
39. Lopez-Abarrategui C, Alba A, Silva ON, et al. Functional characterization of a synthetic hydrophilic antifungal peptide derived from the marine snail *Cenchritis muricatus*. *Biochimie*. 2012;94:968-974.
40. Adolphe M, Pointet Y, Ronot X, Wepierre J. Use of fibroblast cell culture for the study of wound healing drugs. *Int J Cosmet Sci*. 1984;6:55-58.
41. Bucalo B, Eaglstein WH, Falanga V. Inhibition of cell proliferation by chronic wound fluid. *Wound Repair Regen*. 1993;1:181-186.
42. Park SG, Shin H, Shin YK, et al. The novel cytokine p43 stimulates dermal fibroblast proliferation and wound repair. *Am J Pathol*. 2005;166:387-398.
43. Mansbridge JN, Liu K, Pinney RE, Patch R, Ratcliffe A, Naughton GK. Growth factors secreted by fibroblasts: role in healing diabetic foot ulcers. *Diabetes Obes Metab*. 1999;1:265-279.
44. Raghov R. The role of extracellular matrix in post inflammatory wound healing and fibrosis. *FASEB J*. 1994;8:823-831.
45. Smith KP, Zardiackas LD, Didlake RH. Cortisone vitamin A and wound healing: the importance of measuring wound surface area. *J Surg Res*. 1986;40:120-125.
46. Flanagan M. Wound measurement: can it help us to monitor progression to healing. *J Wound Care*. 2003;12:189-194.

How to cite this article: Ulagesan S, Sankaranarayanan K, Kuppusamy A. Functional characterisation of bioactive peptide derived from terrestrial snail *Cryptozonia bistrialis* and its wound-healing property in normal and diabetic-induced Wistar albino rats. *Int Wound J*. 2018;15:350–362. <https://doi.org/10.1111/iwj.12872>